International Journal of Innovative Technologies
WWW.IJITECH.ORG
ISSN 2321-8665
Volume.06, Issue.01,
January-June, 2018,
Pages:0159-0164

Extended Phase Shift Control of Multiple Renewable Sources with Power Sharing Capability in Micro Grid System

TIPIRISETTI RAKESH[1], SURESH[2]
[1]PG Scholar, TKR College of Engineering and Technology, India, E-mail: traki284@gmail.com.
[2]Assistant Professor, TKR College of Engineering and Technology, India, E-mail: suresh.g151189@gmail.com.

Abstract: The extended phase shift controller boosts the voltage of the low voltage renewable sources which is connected to DC bus in turn connected to AC grid through inverter. Multiple renewable sources such as PVA (Photo Voltaic array), Fuel cell, Battery and super capacitor generate power at low voltages which are stepped up using extended phase shift controller separately for each source. The complete design and analysis is carried out in MATLAB Simulink with all graphical representations.

Keywords: Maximum Power Point(MPP), PVA (Photo Voltaic Array), Fuel Cell.

I. INTRODUCTION

Photovoltaic (PV) power-generation systems are becoming increasingly important and prevalent in distribution generation systems. A conventional centralized PV array is a serial connection of numerous panels to obtain higher dc-link voltage for main electricity through a dc–ac inverter [1], [30]. Unfortunately, once there is a partial shadow on some panels, the system's energy yield becomes significantly reduced [2]. An ac module is a microinverter configured on the rear bezel of a PV panel [1]–[3]; this alternative solution not only immunizes against the yield loss by shadow effect, but also provides flexible installation options in accordance with the user's budget [4]. Many prior research works have proposed a single-stage dc– ac inverter with fewer components to fit the dimensions of the bezel of the ac module, but their efficiency levels are lower than those of conventional PV inverters. The power capacity range of a single PV panel is about 100 W to 300 W, and the maximum power point (MPP) voltage range is from 15 V to 40 V, which will be the input voltage of the ac module; in cases with lower input voltage, it is difficult for the ac module to reach high efficiency [3]. However, employing a high step-up dc–dc converter in the front of the inverter improves power-conversion efficiency and provides a stable dc link to the inverter. When installing the PV generation system during daylight, for safety reasons, the ac module outputs zero voltage [4], [5]. Fig1 shows the solar energy through the PV panel and micro inverter to the output terminal when the switches are OFF. When installation of the ac module is taking place, this potential difference could pose hazards to both the worker and the facilities.

A floating active switch is designed to isolate the dc current from the PV panel, for when the ac module is off-grid as well as in the nonoperating condition. This isolation ensures the operation of the internal components without any residential energy being transferred to the output or input terminals, which could be unsafe. In order to realize power distribution between energy generation systems and storage systems in micro grids, various bidirectional DC–DC converters (BDCs) have been proposed as an everlasting key component to interface between a high-voltage bus, where an energy generation system such as a fuel cell stack or a photovoltaic array is installed, and a low-voltage bus, where usually an energy storage system such as a battery or a super capacitor is implemented, as shown in Fig1 [1]. Generally, BDC is divided into nonisolated type [12], [13] and isolated type[1], [4], and galvanic isolation for BDC is required for flexibility of system reconfiguration and meeting safety standards [14], [17]. State-of-the-art isolated bidirectional DC–DC converter (IBDC) is based on the single-phase and H-bridge topology with a high-frequency isolation transformer. Fig. 2 depicts a typical configuration of IBDC. Compared to traditional DC–DC converter circuits, this converter has many advantages, such as electrical isolation, high reliability, easy to realize soft-switching control, and bidirectional energy flow [4]–[6].

Generally, there are mainly two kinds of control methods for such topology: traditional pulsewidth modulation (PWM) control [7]–[9] and phase-shift control. In traditional PWM control, the cross-connected switch pairs in H-bridge (H1), such as (S1,S4) and (S2,S3), are switched in turn to transform the high-voltage V1 from DC to AC, the switches (Q1–Q4) in H-bridge (H2) are turned OFF and the current conducts only through the diodes (M1–M4) to transform the voltage from AC to DC, so the power is transferred from V1 side to V2 side. In the reverse power flow, the states of S1–S4 and Q1–Q4 are exchanged. This control method is simple and easy to implement, but it has poor dynamic performance. And the AC output voltage can only be lower than DC input voltage in H-bridge inverter, so its regulating range of voltage is limited. In TPS control [4]–[6], the cross-connected switch pairs in both H-bridges (H1 and H2) are switched in turn to generate phase-shifted transition square waves to the transformer's primary and secondary sides. And the

corresponding phase shift changes the voltage across the transformer's leakage inductor to manipulate the power flow direction and magnitude. This control method is attracting more and more attention due to its advantages such as small inertia, high dynamic performance, easy to realize soft-switching control, and so on. But in this method, the control of the power flow is dependent on transformer's leakage inductor that result in great circulating power andcurrent stress when the value of V1/nV2 deviate far from 1, where n is turns' ratio of the transformer. And then, the loss in power devices and magnetic components is increased and the efficiency of converter is reduced. In order to improve the performance of the IBDC, various control methods were explored [1]–[5].

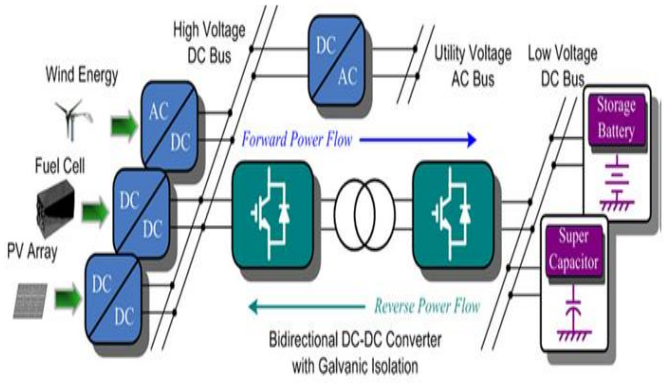

Fig. 1. Test system with extended phase shift control.

In some of these studies [1], [2], the duty ratio of the driving signals of each semiconductor device is variable, and should be calculated online, that increases the complexity of the control. Some studies are focused on how to extend the soft-switching range [3] or eliminate reactive power [4], the detailed analysis of steady characteristics is not conducted. In [5], a novel phase-shift dual-half-bridge converter with an adaptive inductor was proposed. It utilizes an adaptive inductor as the commutation inductor to adapt to the change of the output power, which results in strict requirements of the coiling method of inductor and the complexity of the control. And it is mainly improvement of hardware design; the control method of the proposed converter is still TPS control. In view of the study situation mentioned above, this paper points out a phenomenon of power back flow in traditional phase-shift control, and analyzes the effects which back flow power act on power circulating flow and current stress. On this basis, the paper presents a novel extended-phase-shift control of IBDC for power distribution in microgrid. Different from the control methods mentioned above, this method adds another degree of freedom to the converter by adjusting the time sequence between the driving signals of diagonal semiconductor switches, e.g.,(S1, S4) in Fig2. It not only has smaller power circulating flow and current stress, but also expands regulating range of transmission power and enhances regulating flexibility.

II. MODELING OF PVA

For efficient renewable power generation PVA is used to generate power from solar irradiation. As the load demand is increasing day by day the power generation also has to be increased, but due to the traditional way of power generation is causing global warming. Due to this the efficiency of the PVA has to be increased by adding silicon surface on the panel. And also employ MPPT techniques to track maximum power during any irradiation and atmospheric conditions. The design of PVA is done in MATLAB with Simulink block, with mathematical representation. Voltage of PVA completely depends on solar irradiation (Sx) and ambient temperature (Tx). PVA (Photo voltaic array) is a combination of series and parallel solar cells arranged in an array to generated the required voltage and current. Each series combination of cells can be considered as photo voltaic module. Increase in series cells increases the voltage and increase in parallel cells increases the current capacity. Formulation for voltage of each cell is given below

$$V_C = \frac{AkT_C}{e}\ln\left(\frac{I_{ph}+I_0-I_C}{I_0}\right)-R_S I_C \quad (1)$$

Where, k = Boltzmann constant (1.38 × 10-23 J/oK).
I_c = cell output current, Amp.
I_{ph} = photocurrent
I_0 = reverse saturation current of diode
R_s= series resistance of cell
T_c= reference cell operating temperature
V_c= cell voltage, V.

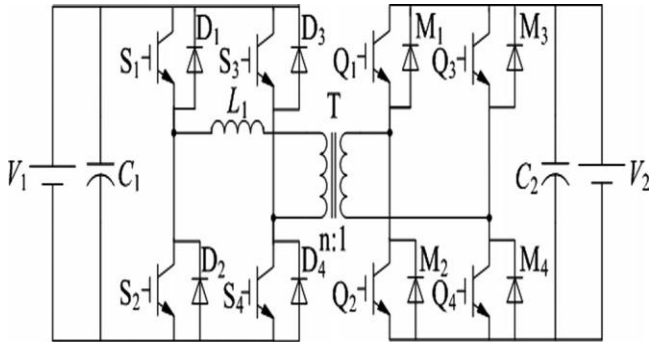

Fig. 2.Extended phase shift control internal circuit.

The Boltzmann constant and the reference temperature have to be in same units ie., either ^{0}C or ^{0}K. The mathematical modeling of the above equation can be constructed using simulink blocks is as below Fig.3.

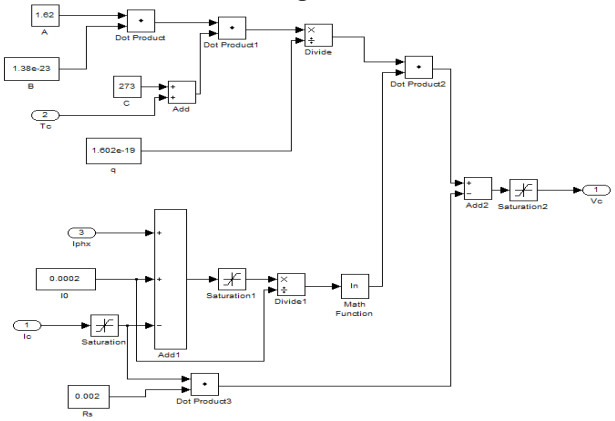

Fig. 3. Simulink model of Vc.

The above design is for a single cell voltage, in order to increase the voltage of the PVA the cell voltage has to be multiplied to a desired values considering each cell voltage as 0.4V. So, the number of series connected cells (Ns) can be calculated as

$$N_s = Vo/0.4 \quad \textbf{(2)}$$

To get each cell current, the total current output from the dependable source has to be divided by number of parallel connected cells (Np). Therefore, parallel connected cells are considered as

$$N_p = I_o/I_{cell} \quad \textbf{(3)}$$

The representation in simulink is taken as shown in Fig.4.

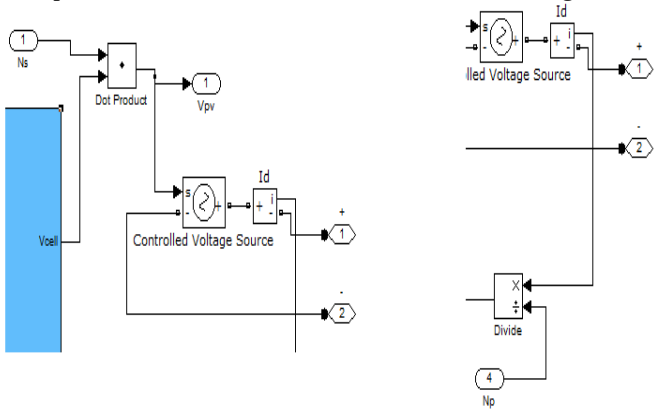

Fig. 4. Simulink modeling of Ns & Np.

For the calculation of Vcx(cellvoltage) and Iphx (Photocurrent) we need correction factors C_{TV} C_{TI} C_{SV} C_{SI}. The formulation is given as

$$V_{CX} = C_{TV} C_{SV} V_C$$
$$I_{phx} = C_{TI} C_{SI} I_{ph} \quad \textbf{(4)}$$

The correction factors are given as

$$C_{TV} = 1 + \beta_T (T_a - T_x)$$
$$C_{TI} = 1 + \frac{\gamma_T}{S_C}(T_x - T_a) \quad \textbf{(5)}$$
$$C_{SV} = 1 + \beta_T \alpha_S (S_x - S_C)$$
$$C_{SI} = 1 + \frac{1}{S_C}(S_x - S_C) \quad \textbf{(6)}$$

Where, β_T = 0.004 and γ_T = 0.06
T_a = reference temperature
T_x = ambient temperature
S_c = reference solar irradiation
S_x = ambient solar irradiation

The values of T_x and S_x changes depending upon the Sun rays which change continuously and unpredictably. The effect of change in solar irradiation varies the cell photocurrent and also the cell voltage (Vc). Let us consider the initial solar irradiation is I_{sx1}& the increase of the irradiation is I_{sx2} which in turn increases the temperature from T_{x1} to T_{x2}, photocurrent from I_{phx1} to I_{phx2}. The mathematical modeling of the correction factors in simulink is given below Fig.5.

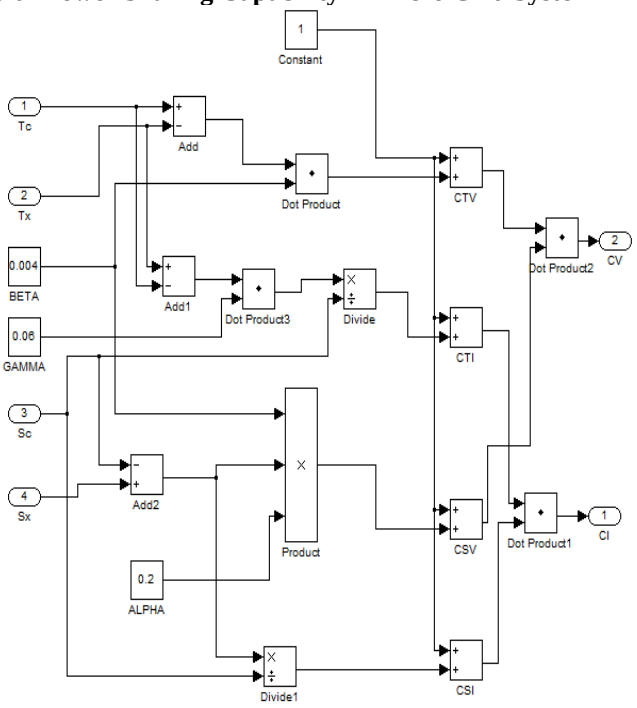

Fig. 5. CI & CV modeling.

Depending upon the solar irradiation and temperature the values of CV & CI are calculated which is fed to Vc block to get the cell voltage value as shown below Fig.6.

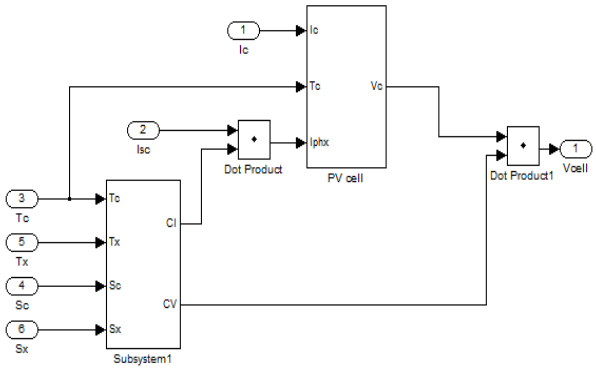

Fig. 6. Combined diagram of CV CI &Vc mathematical models.

The total system diagram of the PVA with all the mathematical formulation are put into a subsystem to make it clear and understandable. The output of the Vc multiplied with the Ns constant block defining the total voltage of the combined cells of the PVA is fed to the voltage controlled voltage source block so as to generate the required voltage. A diode is connected in series at the positive terminal of the PVA to avoid reverse currents passing into the PVA. To reduce the ripples a capacitor can be added later after the diode in parallel as the capacitor doesn't allow sudden change of voltages dV/dt. The complete PVA module with internal block construction is shown in the fig.7 below

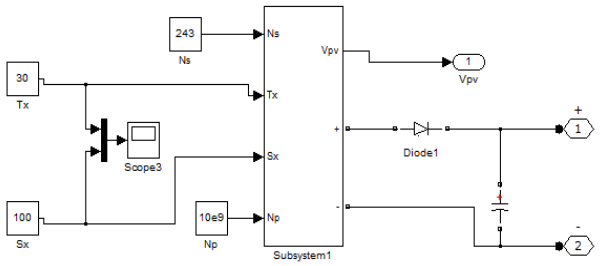

Fig. 7. Complete diagram of PVA.

III. OPERATIONPRINCIPLEOFEXTENDED-PHASE-SHIFTCONTROL

In order to significantly decrease the backflow power of the converter, vh1 should not be confined to square waveforms with 50% duty ratio. For example, if S1 and S4 do not have the same driving signal but have a phase-shift ratio of D1,as shown in Fig. 8, the transformer primary voltage will emerge as a three-level instead of the traditional two-level. Then the behaviors of iL will also be changed: the backflow-appearance time ($t = t_0 \sim t_0$ and $t = t_2 \sim t_2$) in Fig. 8 are divided into two intervals ($t = t_0 \sim t_1$, $t = t_1 \sim t_1$ and $t = t_3 \sim t_4$, $t = t_4 \sim t_4$) in Fig.8, respectively. And the transformer primary voltage vh1 = 0, i.e., backflow power is 0, when $t = t_0 \sim t_1$ and $t = t_3 \sim t_4$.Sothe backflow power is decreased for a given transmission power. In the reverse power flow, we just need to exchange the operating states of the H-bridges H1 and H2.In Fig. 8, D1 is the phase-shift ratio between the driving signals of S1 and S4 or S 2 and S3 in H-bridge H1, we defined its inner phase-shift ratio, where $0 \le D1 \le 1$. D2 is the phase-shift ratio between the primary and secondary voltages of the isolation transformer, we defined its outer phase-shift ratio, where $0 \le D2 \le 1$ and $0 \le D1+D2 \le 1$. In fact, compared to theTPS control, there is not only the outer phase-shift ratio but also the inner phase-shift ratio in the proposed EPS control, which will decrease the current stress, expands regulating range of transmission power and enhances regulating flexibility.

Mode 1 (t_0–t_1): Fig. 8(a) shows the equivalent circuit for the mode 1. Just before t0,S2 and S3 are conducting. The current iL is in negative direction. At t0,S3 is turned OFF and S4 is turnedON at zero current, and D4 starts to conduct. On the secondary side, the current is carried from L to V2 by M2 and M3.The voltage across L is clamped at nV2, and the current iL decreases linearly. This mode ends up when S2 is turned OFF. During this mode, the current of L.

Mode 2 (t_1–t_1): Fig. 8(b) shows the equivalent circuit for mode 2. If current iL is still in negative direction at t1 then at t1,S2 is turned OFF and S1 is turned ON at zero current, iL is carried from L to V1 by D1 and D4. On the secondary side, the current is carried from L to V2 by M2 and M3. The voltage across L is clamped at V1+nV2, and iL still decreases linearly.This mode ends up with iL decreasing to zero.

Mode 3 (t_1–t_2): Fig. 8(c) shows the equivalent circuit for the mode 3. At t 1, the polarity of iL changes from negative to positive. And because the driving signals of S1,S4,Q2, and Q3 are already on, so S1,S4,Q2, and Q3 start to conduct.The voltage across L is clamped at V1 + nV2, and iL increases linearly. This mode ends up when Q2 and Q3 are turned OFF. During this mode, iL is the same with (2).

Mode 4 ($t_2 – t_3$): Fig. 8(d) shows the equivalent circuit for the mode 4.At t2,Q2 and Q3 are turned off and Q1 and Q4 are turned on at zero current. M1 and M4 start to conduct. The voltage across L is clamped at V1–nV2, and iL still increases linearly due to $V1 \ge nV2$.

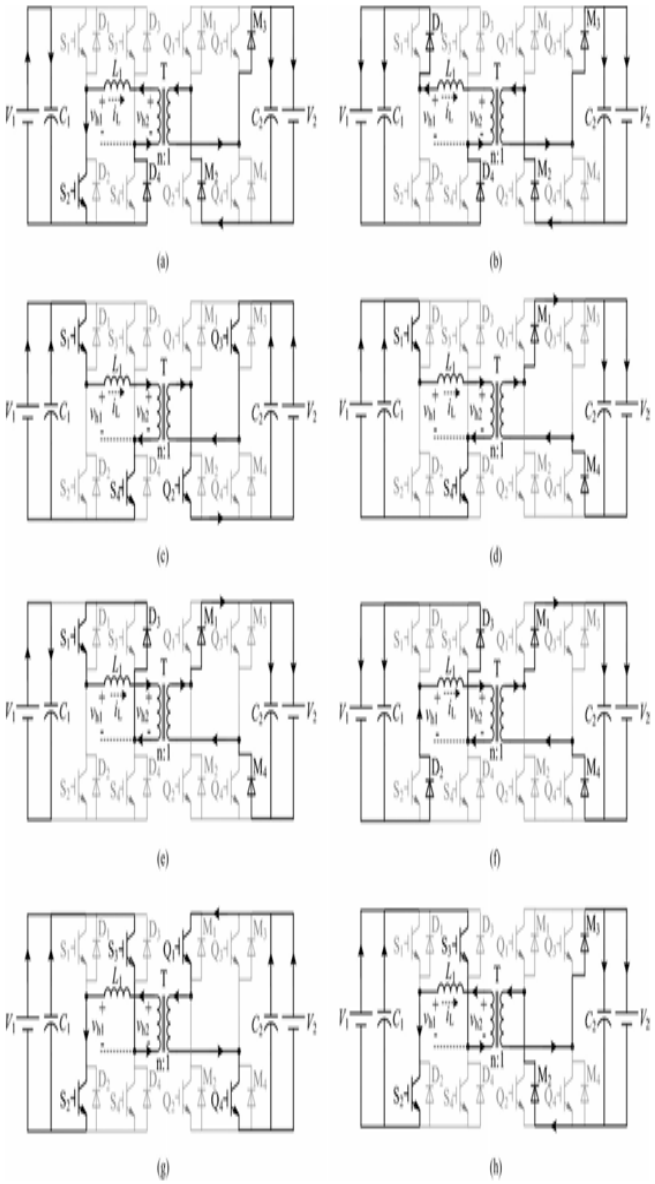

Fig.8. Operating modes of extended phase shift controller.

Mode 5 ($t_3 – t_4$): Fig. 8(e) shows the equivalent circuit for mode 5.At t3,S4 is turned OFF and S3 is turned ON at zero current, D3 starts to conduct. On the secondary side, the current is carried from L to V2 by M1 and M4. The voltage across L is clamped at –nV2, and the current iL decreases linearly. This mode ends up when S1 is turned OFF.

Mode 6 ($t_4 - t_4$): Fig. 8(f) shows the equivalent circuit for mode 6. If current iL is still in positive direction at t4, then at t4,S2 is turned OFF and S1 is turned ON at zero current, iL is carried from L to V1 by D2 and D3. On the secondary side, the current is carried from L to V2 by M1 and M4. The voltage across L is clamped at –V1–nV2, and iL still decreases linearly. This mode ends up with iL decreasing to zero.

Mode 7 (t_4–t_5): Fig. 8(g) shows the equivalent circuit for the mode 7.At t 4, the polarity of iL changes from positive to negative. And, because the driving signals of S2,S3,Q1, and Q4 are already ON, so S2,S3,Q1, and Q4 start to conduct.The voltage across L is clamped at –V1–nV2, and iL increases linearly. This mode ends up when Q1 and Q4 are turned OFF.During this mode, iL is the same with (5).

Mode 8 ($t_5 - t_6$): Fig. 8(h) shows the equivalent circuit for the mode 8.At t5,Q1 and Q4 are turned OFF and Q2 and Q3 are turned ON at zero current. M2 and M3 start to conduct. The voltage across L is clamped at –V1+nV2, and iL still increases linearly due to V1 ≥ nV2. This mode ends up when S3 is turnedOFF.

IV. SIMULINK RESULTS AND OUTPUTS

Simulation results of this paper is as shown in bellow Figs.9 to 11.

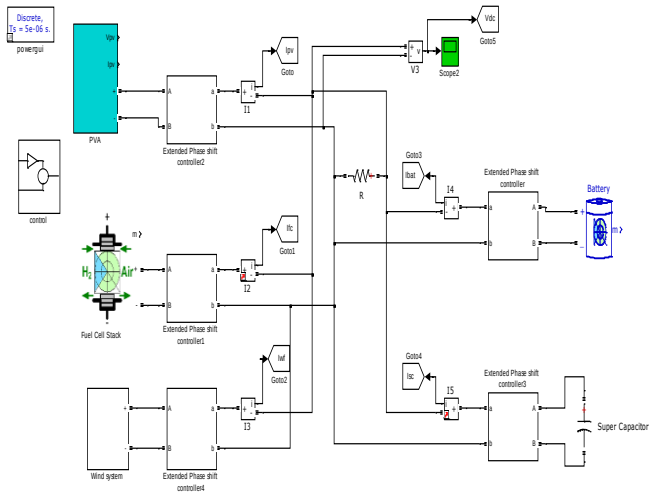

Fig. 9.Simulink test system with extended phase shift controllers.

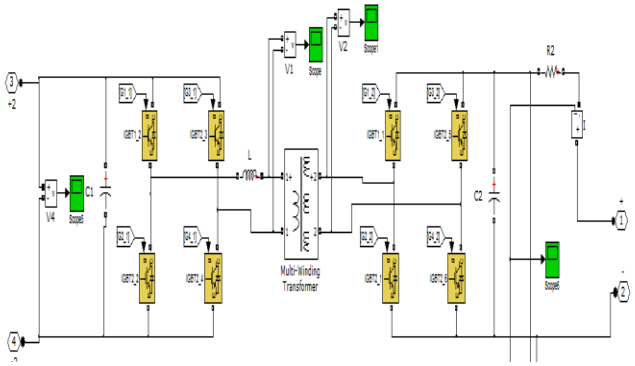

Fig. 10. Extended phase shift controller.

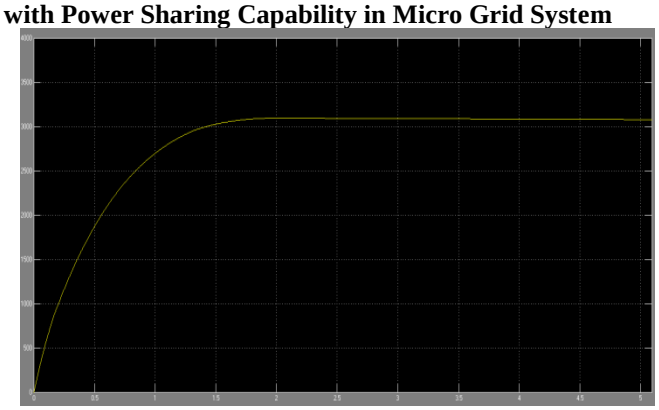

Fig. 11. DC bus voltage.

V. CONCLUSION

IBDC is an everlasting key component to realize power distribution between energy generation systems and storage systems in microgrids. In order to overcome the inherent disadvantages of TPS control of IBDC, a novel EPS control is proposed for power distribution in microgrid in this paper. From the theoretical analysis and the experiments, it can be found that EPS control has the following features: 1) EPS control expands regulating range of transmission power and enhances regulating flexibility. 2) EPS control reduces power-circulating flow, and thus reduces conduction losses and improves the system efficiency. 3) EPS control reduces current stress, and thus reduces switching losses and prolongs the service life of devices. For the same power level, the devices can be selected with lower stress levels, which saves the cost. 4) EPS control is simple in principle and easy to implement.

VI. REFERENCES

[1]R.H.Lasseter,"Smartdistribution:Coupledmicrogrids,"Proc .IEEE.,vol.99,no.6,pp.1074–1082,Jun.2011.

[2]P.Tenti,H.K.M.Paredes,andP.Mattavelli,"Conservativepow ertheory,aframeworktoapproachcontrolandaccountabilityissue sinsmartmicrogrids,"IEEETrans.PowerElectron.,vol.26,no.3,p p.664–673,Mar.2011.

[3]R.Majumder,A.Ghosh,G.Ledwich,andF.Zare,"Powermana gementandpowerflowcontrolwithbacktobackconvertersinautili tyconnectedmicrogrid,"IEEETrans.PowerSystem.,vol.25,no.2 ,pp.821–834,May2010.

[4]A.K.Abdelsalam,A.M.Massoud,S.Ahmed,andP.N.Enjeti," Highperformanceadaptiveperturbandobserve MPPTtechniquef orphotovoltaicbasedmicrogrids,"IEEETrans.PowerElectron.,v ol.26,no.4,pp.1010–1021,Apr.2011.

[5]J.M.Guerrero,J.C.Vasquez,J.Matas,M.Castilla,andL.G.Vic una,"Controlstrategyforflexiblemicrogridbasedonparallelline-interactiveUPSsystem,"IEEETrans.Ind.Electron.,vol.56,no.3, pp.726–736,Mar.2009.

[6]J.Y.Kim,J.H.Jeon,S.K.Kim,C.Cho,J.H.Park,H.M.Kim,and K.Y.Nam,"Cooperativecontrolstrategyofenergystoragesystem andmicrosourcesforstabilizingthemicrogridduringislandedope ration,"IEEETrans.PowerElectron.,vol.25,no.12,pp.3037–3048,Dec.2010.

[7]J.-H.Jeon,J.Y.Kim,H.M.Kim,S.-K.Kim,C.Cho,J.M.Kim,J.-B.Ahn,andK.Y.Nam,"Developmentofhardwareintheloopsimu lationsystemfortestingoperationandcontrolfunctionsofmicrogr

id,"IEEETrans.PowerElectron.,vol.25,no.12,pp.29192929,Dec.
2010.
[8]T.F.Wu,K.H.Sun,C.L.Kuo,andC.H.Chang,"Predictivecurren
tcontrolled5kWsinglephasebidirectionalinverterwithwideinduct
ancevariationfordcmicrogridapplications,"IEEETrans.PowerEle
ctron.,vol.25,no.12,pp.3076–3084,Dec.2010.
[9]M.G.MolinaandP.E.Mercado,"Powerflowstabilizationandco
ntrolofmicrogridwithwindgenerationbysuperconductingmagneti
cenergystorage,"IEEETrans.PowerElectron.,vol.26,no.3,pp.910
–922,Mar.2011.